

Hybrid MV-LV Power Lines and White Light Emitting Diodes for Triple-Play Broadband Access Communications

M. Kavehrad, FIEEE

W.L. Weiss Professor, Department of Electrical Engineering, Center for Information & Communications Technology Research (CICTR)

The Pennsylvania State University

P. Amirshahi

Ph.D. Candidate, Department of Electrical Engineering, Center for Information & Communications Technology Research (CICTR)

The Pennsylvania State University

Abstract

Home users are in need for broadband-communications access globally. Broadband power-line transmission has advanced throughout the last decade, and it is going to be a mature last-mile access in the near future. Meanwhile, indoor optical wireless communications through lighting LEDs has been investigated recently. Suitable channel models are proposed for each of these systems, and the corresponding transmission capacity values are calculated. It is shown that a combination of these two technologies makes an efficient method for fulfilling the premise of broadband access for home networking while providing efficient and low-cost lighting.

I. Introduction

The increasing interest in modern multimedia applications, such as broadband Internet, HDTV, etc. requires new last-mile-access techniques for connecting private premises to a communication backbone. One promising technology, broadband over power-lines (BPL), uses electric power lines

as a high-speed digital data channel to connect a group of private users to a very-high-data-rate backbone such as fiber optic. The lines in a power delivery network can be categorized based on several criteria. Depending on line voltage, high voltage (HV), medium voltage (MV), and low voltage (LV) grids are typically defined. Most HV-MV transformer locations are equipped with a high-speed fiber connection. Therefore, MV lines can act as the first pipeline of high-speed connection from the backbone to the home users.

Channel characteristics of medium voltage overhead power-line grids, a common type of grid in the United States, were investigated in detail by the authors in “Transmission Channel Model and Capacity” and “Medium Voltage Overhead Power-Line Broadband Communication.” It is shown that although the overhead power-line grid is a very low-loss medium, it may suffer from very deep fading caused by a multipath scenario. Mismatch at the branches of the power-line network reflects signals back and creates several signal paths from a transmitter to a receiver. In the same papers, Shannon capacity limits of overhead MV-lines

channels have been investigated. It is shown that the overhead power-line grid network has a high-capacity limit compared to other similar wireline structures such as cable and twisted pairs.

Each home is equipped with electricity by means of an LV power-line grid. LV lines are distributed to each power plug in every room in a house. More than 99 percent of homes in the United States have access to electricity, whereas connectivity level is far less for cable and phone lines. Thus, a combination of MV and LV power lines can be an appropriate candidate for providing broadband access to every home in the country. The characteristics of LV power lines are very well known, and there are a variety of research activities in this area to exploit different features of LV grids. One of the most recent and comprehensive efforts of this kind was undertaken by Galli and Banwell.^{3,4} This research uses multi transmission line (MTL) theory, also used in “Transmission Channel Model and Capacity,” to characterize the indoor LV–power-line networks.

Indoor wireless connectivity is always appealing to consumers because of its ease of use. One of the conventional wireless access systems is Wi-Fi. But these systems and similar other wireless schemes suffer from so many shortages, including interference, not providing quality of service (QoS), adequate coverage, etc.

A better candidate for wireless home networking is optical wireless. Use of conventional lasers for optical indoor communications has not been feasible as yet because of the high cost of laser sources. Instead of lasers, LEDs can be used as communications transmitters connected to electric grid, receiving high-bit-rate signals via BPL.

Recently, white LEDs emerged in the market and are considered as future “lamps.” Apparently, in the near future, the incandescent and fluorescent lamps will be replaced by the low cost, efficient and miniature white LEDs. Researchers pledge that by 2012, these devices will reach seven watts and 1000 luminescence. This is brighter than a 60-watt bulb, yet draws a current provided by four D-size batteries.⁵ A Japanese research team suggested using the same white LEDs not only for lighting the homes but also

as light sources for wireless in-house communications.⁶ Using this new and developing technology along with MV-LV–power-line communications can create a revolution in the area of consumer networking because of its efficiency and affordability.

In this paper, we investigate the abilities of each of these technologies for providing broadband communications. In section II, a brief review of channel characteristics of MV–power-line systems is cited. Section III provides transfer functions of a typical LV system and its associated capacity. White–LED communications systems and their characteristics are described in section IV. Concluding remarks and references end the discussion.

II. Overhead MV Power-Line Channel Model and Its Capacity

The channel transfer function of a matched transmission power line follows (1–2)

$$V(l) = H(f)V(0) \tag{1}$$

$$H(f) = e^{-\gamma(f)l} = e^{-\alpha(f)l} e^{-j\beta(f)l} \tag{2}$$

in which $v(0)$ is the voltage at the source and γ is the propagation constant; α , the real part of the propagation constant, is called attenuation constant, and β , the imaginary part of the propagation constant, is called phase constant. To find an exact solution for γ at high frequencies with lossy ground return, several research efforts have been launched since early last century. A more recent investigation in this area is by D’Amore and Sarto, as reported in “A New Formulation of Lossy Groud Return Parameters.” By applying this method, the propagation constant of overhead power-lines can be obtained for frequencies close to 100 MHz.¹

Channel transfer function of a matched transmission power line follows (2). In the case of unmatched junctions, part of a propagating signal gets reflected back to the transmitter at branch junctions because of impedance mismatch, and the remainder travels through.⁸ The propagation along a wire follows (2), so one can easily express the multipath network channel model as

$$H(f) = \sum_{i=1}^N g_i e^{-\alpha(f)d_i} e^{-j\beta(f)d_i} \tag{3}$$

where N is the number of significant arrived paths at the receiver, d_i is the length of i^{th} path and g_i is the weighting factor of the i^{th} path. Coefficient g_i is very well defined in “Measurements of the Communications Environment.”

For example, using the described method, we simulate the complex network shown in “Transmission Channel Model and Capacity.” In this network, we have three branches between a transmitter and a receiver, which are by one kilometer apart. Each end of these branches is an open-circuit, so reflection factor at each end is in unity. Also, we have assumed that the transmitter and receiver impedances are matched to those of the lines. Channel frequency and impulse responses of this system are shown in *Figure 1(a)* and *(b)*. Our simulation results show 12 paths are dominant and in *Figure 1(b)*; 12 pulses with different arrival times are visible. The maximum delay spread of this channel is approximately three microseconds. *Figure 1(c)*

illustrates capacity limits of this channel. For evaluating channel capacity, we chose a uniform of -105 dBm/Hz as a representative average background-noise spectral-density level. Referring to “A multipath model for the power-line channel,” this value is a conservative average estimate of a practical background noise level for MV-power lines. According to *Figure 1(c)*, the average capacity in this network with a ten dBm launched transmit power level at 50 MHz band is about 400 Mbps.

III. LV Power-Line Transfer Function and Its Capacity

As in “Transmission Channel Model and Capacity,” characteristic of LV-power-line grids have to be utilized by means of MTL theory. As it is mentioned in “A Novel Approach to the Modeling of the Indoor Power Line Channel—Part I,” the conventional two-conductor transmission line (TL) is not able to

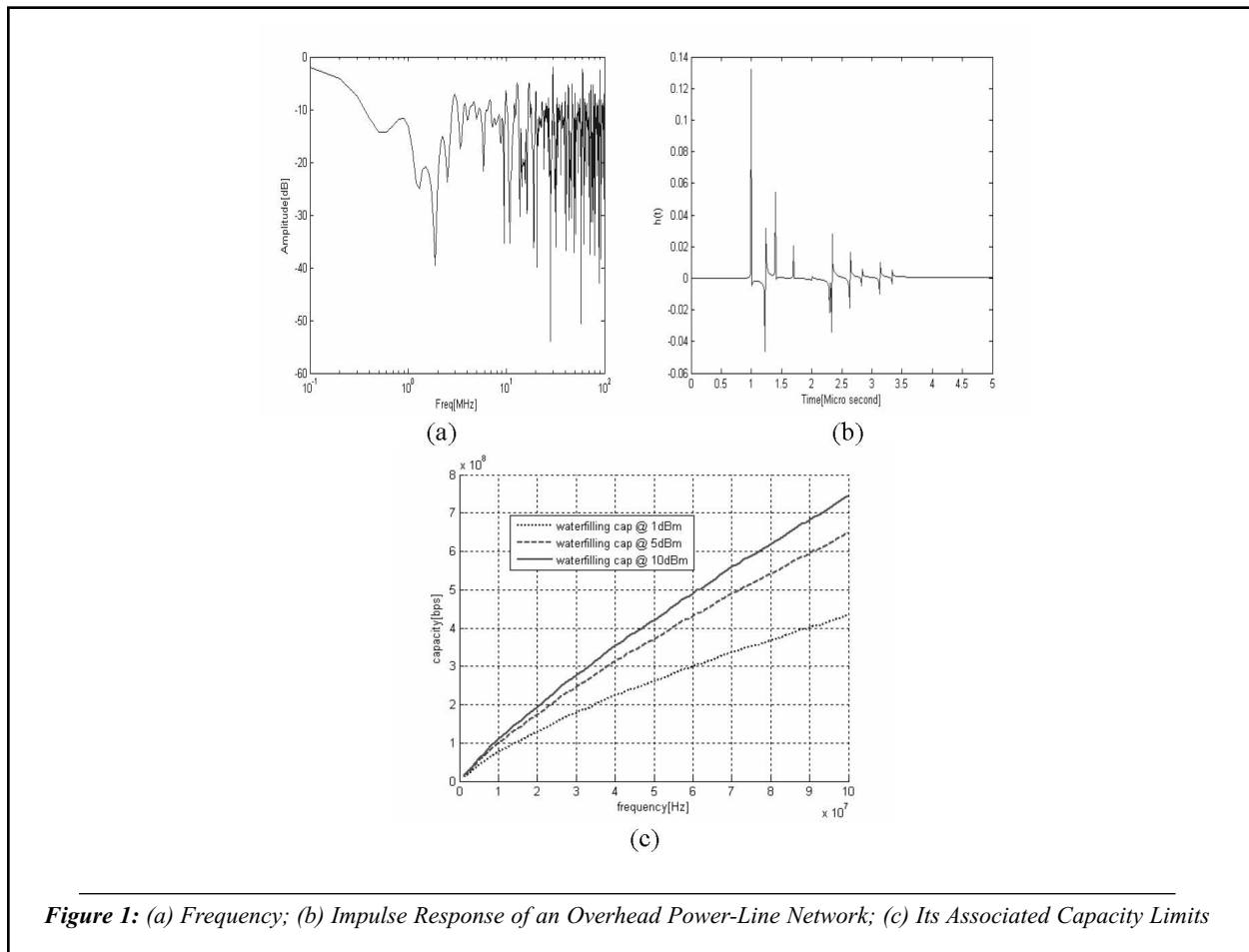


Figure 1: (a) Frequency; (b) Impulse Response of an Overhead Power-Line Network; (c) Its Associated Capacity Limits

explain the physical reasons of propagation behavior on LV-power-line networks completely. For an MTL with $(n+1)$ conductors placed parallel to the x -axis, there are n forward- and n reverse-traveling waves with respective velocities. These waves can be described by a coupled set of $2n$, first-order, matrix partial differential equations that relate the line voltage $V_i(x, t)$, $i=1, 2, \dots, n$, and line current $I_i(z, t)$, $i=1, 2, \dots, n$. Each pair of forward- and reverse-traveling waves is referred to as a mode. This approach for modeling LV-power-line networks is described in comprehensive details in “A Novel Approach to the Modeling of the Indoor Power Line Channel—Part I” and “Part II.” Using methods and algorithms mentioned in this research, we simulated the channel configuration shown in *Figure 7* of “Part I.” The result of frequency response and impulse response of such a channel is illustrated in *Figure 2(a)* and *(b)*. The average loss of this system is more than that of MV lines; however, it exhibits less resonance than typically found on MV lines because of shorter paths. Our

result and results in “Part I” are in agreement. It is seen from the impulse response of *Figure 2(b)* that the maximum delay spread is less than one microsecond and there are four significant paths from transmitter to receiver. The capacity limits of this channel are depicted in *Figure 2(c)*. For evaluation of these limits, we assumed an additive uniform background noise with -120 dBm/Hz as spectral density level. According to “Measurements of the Communications Environment,” the background noise in LV networks has a smaller PSD level than in MV and has an average value around -120 dBm/Hz. It is seen from *Figure 2(c)* that the average capacity in this network with 10 dBm-launched transmit power can reach 600 Mbps at 60 MHz.

IV. White-LED Communications and Its Efficiency

White LEDs are considered strong candidates for the future of lighting technology.¹⁰ The reason is that LEDs offer very favorable characteristics such as

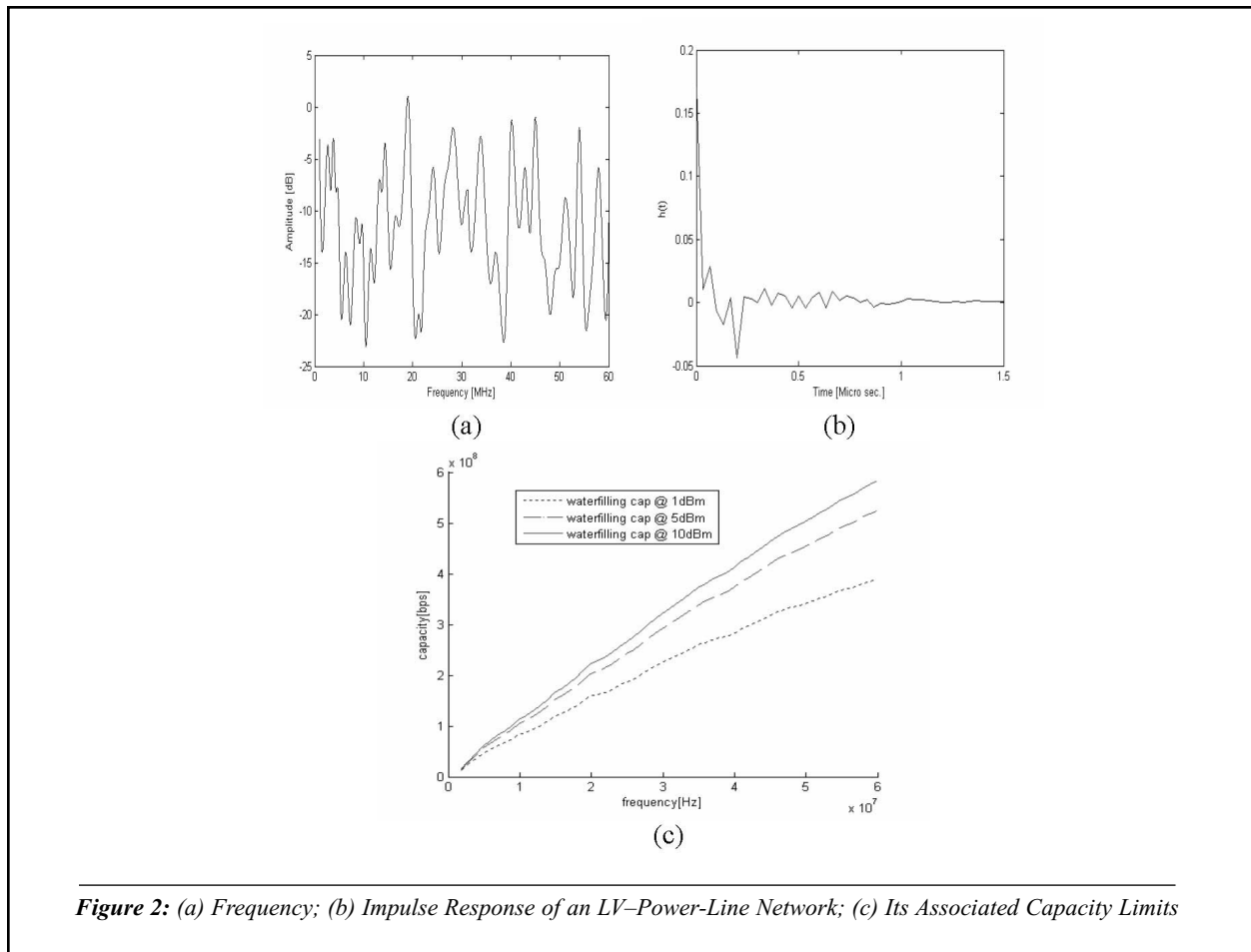


Figure 2: (a) Frequency; (b) Impulse Response of an LV-Power-Line Network; (c) Its Associated Capacity Limits

high brightness, very low power consumption, and high lifetime expectancy. Therefore, it is predicted that in near future, white LEDs will replace the conventional incandescent and fluorescent lamps.

Moreover, LEDs can be used as a wireless communications transmitter. This is not possible for any other kind of lamps in broadband transmissions. This functionality of LEDs as a transmitter is based on a fast response time and modulation of visible light for wireless communications. *Figure 3* shows a very general realization of a visible light communication system using white LEDs. This system is a wireless optical indoor system that uses visible light as a communications carrier. The concept of indoor optical communications has been an active area of research since early 1980s. Most of the research in this area is done based on infrared (IR) as the communication carrier, and nearly all results from these efforts are applicable to any parts of light frequency spectrum.

There are several advantages to using white LEDs for communications over Wi-Fi and IR for indoor communications:

- Installation is easier than most other wireless systems.
- White-LED radiation is not subject to spectrum licensing regulations because it does not cause any electromagnetic interference, whereas there are always concerns in using Wi-Fi or any other RF communications systems in terms of interference from or to other wireless communication systems.

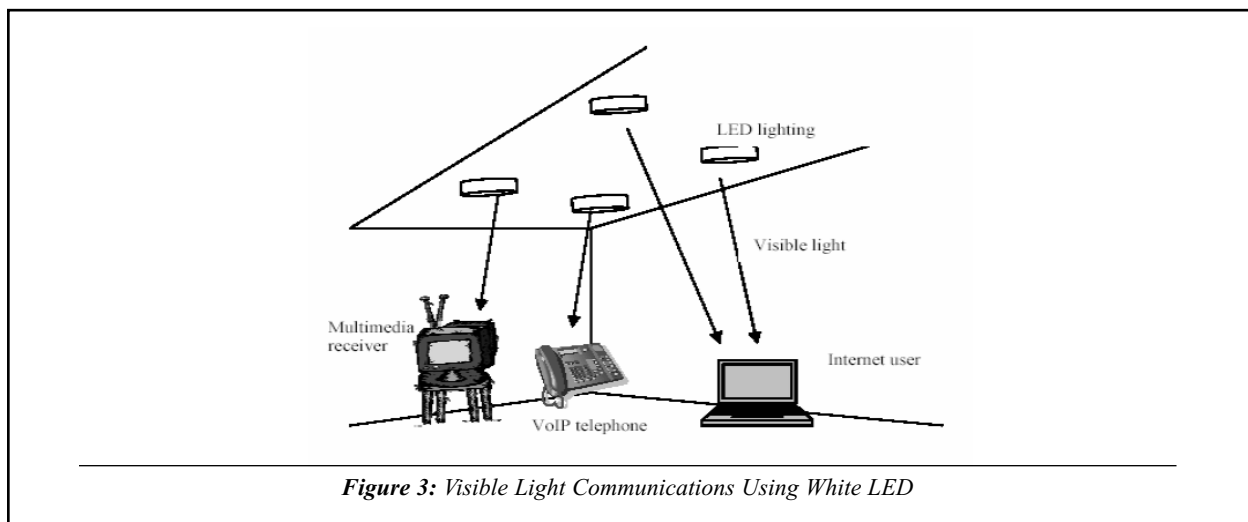
- Different users in different rooms and buildings do not interfere with one another because LED–signal rays do not go through walls; hence, a huge band can be reused many times over in a small area. On the other hand, in Wi-Fi systems, it is possible that different transmitted access-point signals interfere and cause a degraded performance.
- The shadowing effect is so much less compared to directed methods, as LED light fixtures are distributed throughout a room.
- LEDs are less expensive than laser sources used in IR.
- The receiver obtains at least one strong line of sight (LOS) signal as the transmitters are on the ceiling. This is not the case in most IR transmission situations.

For any optical-transmitter–half-power (HP) angle and for any optical receiver, field of view (FOV) is defined. Half-power angle is the highest angle that the transmitter can illuminate, and FOV is the highest angle that the receiver can receive signal rays from. The mathematical definitions of these parameters are given by *Equations (4) and (5)*.

$$FOV = \tan^{-1}\left(\frac{r_1}{H}\right) \quad (4)$$

$$HP = \tan^{-1}\left(\frac{r_2}{H}\right) \quad (5)$$

where r_1 , r_2 , and H are shown in *Figure 4*.



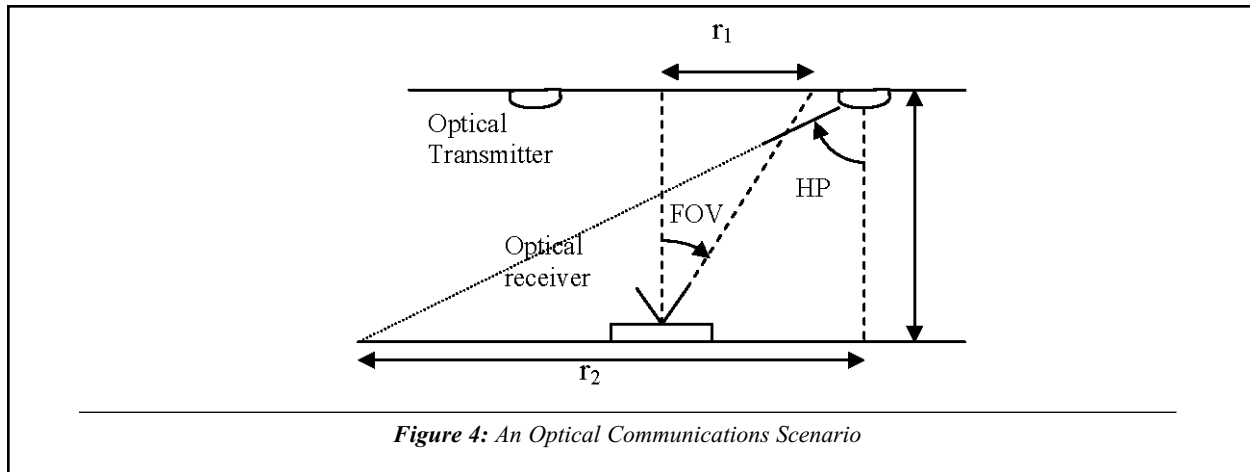


Figure 4: An Optical Communications Scenario

To illuminate a room with white LED, we need to use several LEDs. For modeling purposes, we used the scheme shown in Figure 5. In this model room, nine LED lamps—which consist of several LEDs—are employed with two-meters spacing between the lamp rows on the ceiling and a one-meter distance to the walls. As is shown in “Fundamental analysis for visible light communications using LED lights,” to have a uniform illumination anywhere in the room, the HP angle has to be greater than 70 degrees.

The illumination coverage area of the center lamp is shown in Figure 5 by a dashed circle. The receiver should be designed in a way that its FOV is high enough to at least receive a LOS-signal ray from

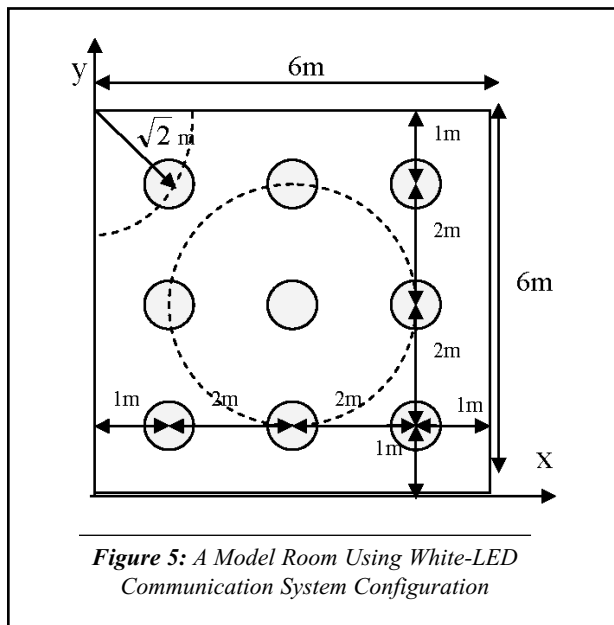


Figure 5: A Model Room Using White-LED Communication System Configuration

one transmitter. In this way, there would be no blind spot in the room. The nearly blind spots in the room are near the corners. According to Figure 5, if the receiver’s coverage area radius is greater than $\sqrt{2}$ meters, receivers at the corners will at least receive one LOS signal from the closest transmitter. If we assume the room height is three meters, this coverage area will correspond to an FOV equal to

$\tan^{-1}(\frac{\sqrt{2}}{3}) \approx 25$ degrees. Therefore, the design for the receiver needs an FOV equal to or greater than 25 degrees. Jivkova and Kavehrad in “Power-Efficient Multispot-Diffuse Multiple-Input-Multiple-Output Approach to Broadband Optical Wireless Communications” have designed an efficient receiver configuration for a FOV of 25 degrees. According to this research, a greater FOV needs more complexity and a greater receiver area. In the same paper, the authors investigated different scenarios of wireless optical communications for covering an indoor space. In this paper, they argue that an FOV of approximately equal to 30 degrees can optimize the link budget of the system both in cellular schemes, like white LED, and diffusing multispot regimes.

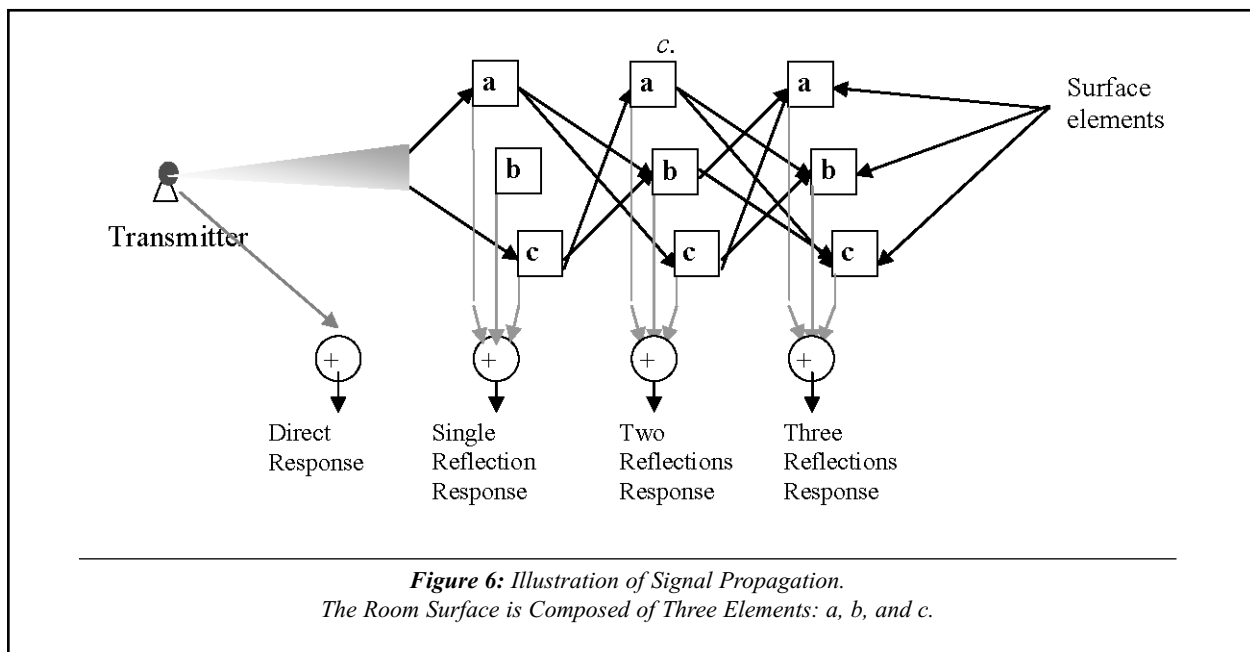
Similar to other communications channels, modeling of wireless optical channels has been a challenge. The very first impulse-response model for these channels was presented in “Wireless in-house data communications via diffuse infra red radiation” by Bapst and Gfeller. Equation (6) is the result of this research.

$$h(t) = \begin{cases} \frac{2\tau_0^2}{t^3 \sin(FOV)} & \tau_0 < t < \frac{\tau_0}{\cos(FOV)} \\ 0 & \text{Elsewhere} \end{cases} \quad (6)$$

where τ_0 is the delay of the shortest path from the transmitter to the receiver. From (6), it is noticed that obtaining a narrower FOV results in a smaller delay spread in the channel. This delay spread is caused by reflections of the optical signals off of the walls. For a room with the dimensions of our model room and with a receiver with 25 degrees FOV, the delay spread cannot exceed two nanoseconds. Furthermore, Equation (6) confirms that reflected signals have so much less power at the receiver compared to LOS-path signals. This causes the impulse response to have a very significant LOS signal and some residual attenuated signals. Because of this fact, some papers—for example, “Wireless optical transmissions with white colored LED for wireless home links”—have assumed that in white-LED communications, the channel consists of only one straight LOS path.

A more rigorous channel modeling process for indoor optical channels was suggested in “MIMO characterization of indoor wireless optical link using a diffuse-transmission configuration.” In this paper, the authors consider up to three signal reflections from the transmitter to the receiver. Their models are used for infrared applications, in which they have their signal source on the floor, aiming a beam at the ceiling. With some modifications, their method can be applied to our system configuration.

The complexity in obtaining channel impulse response is brought about by the multiple paths signals take in traveling from a transmitter to a receiver. This multipath results from reflections off of walls, ceilings, furniture, etc. Room surfaces act as Lambertian reflectors that reflect an incident signal in all directions. Assuming a room surface exposed to a transmitter is made of N surface elements, each reflection produces N-1 new reflections, as illustrated in Figure 6. In this case, the room has assumed to have three elements, and the transmitter has an LOS path to the receiver and two paths to points a and b. The impulse response of any reflection is found by considering all the elements within the receiver FOV. In this example, all the elements are within the receiver FOV. Complexity in calculating impulse response is caused by reflections. Each reflection results in N-1 new reflections. When determining channel impulse response, contribution of each element on a surface within receiver FOV should be considered. Since surfaces do not offer perfect reflection and signal strength is inversely proportional to the distance traveled, a finite number of reflections are considered in obtaining an impulse response.



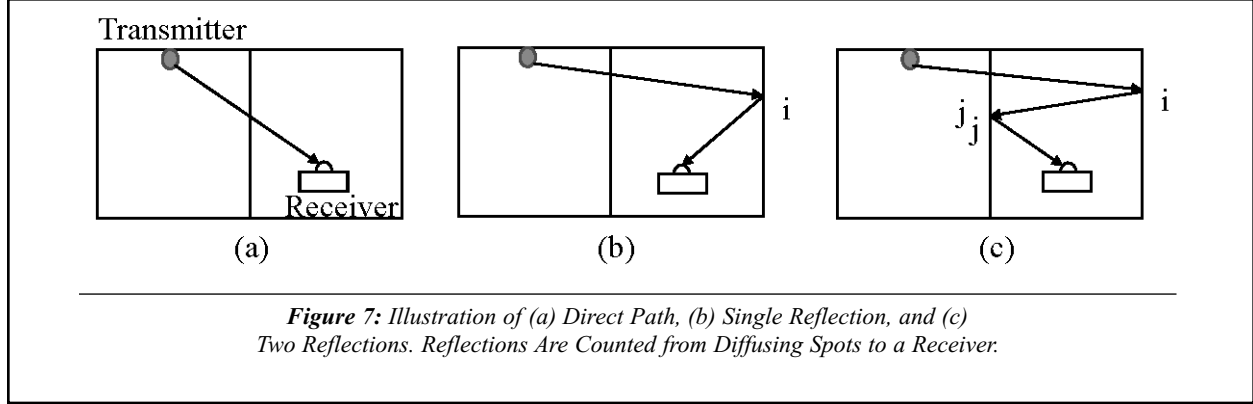


Figure 7: Illustration of (a) Direct Path, (b) Single Reflection, and (c) Two Reflections. Reflections Are Counted from Diffusing Spots to a Receiver.

The radiation pattern of surface elements is assumed a first order Lambertian. They reflect incident light with equal intensity in all directions. Therefore, the intensity at an angle θ from the surface norm is proportional to $\cos(\theta)$.

The line-of-sight response $h^0(t)$, when source T is within the FOV of receiving element R, can be expressed as¹⁵

$$h_{TR}^0(t) = \frac{\cos(\varphi_{TR}) \cdot \cos(\theta_{TR}) \cdot A_R}{\pi R_{TR}^2} \delta\left(t - \frac{R_{TR}}{c}\right) \quad (8)$$

where $\cos(\varphi_{TR})$ is equal to dot product of two unit vectors. The first one is perpendicular to T, and the second one originates from R and extends toward T. The θ_{TR} is the angle between a vector perpendicular to R and a vector along the straight line, connecting T and R. A_R is the receiving element area, R_{TR} is the distance between T and R, and c is the speed of light. The response after a single reflection off an element i is obtained by treating i as a receiver and then as a source as shown in *Figure 7(b)*. The impulse response is given by

$$h_{TR}^1(t) = \frac{\cos(\varphi_{Ti}) \cos(\theta_{Ti}) A_i}{\pi R_{Ti}^2} \rho_i \frac{\cos(\varphi_{iR}) \cos(\theta_{iR}) A_R}{\pi R_{iR}^2} \delta\left(t - \frac{R_{Ti} + R_{iR}}{c}\right) \quad (9)$$

where A_i is the area of the reflecting element i , and ρ_i is its reflectivity. The response resulting from two reflections off elements i first and then off element j is found by extending *Equation (9)* to include impulse response between j and receiver, as illustrated in *Figure 7(c)*, and is expressed as

$$h_{TR}^2(t) = \frac{\cos(\varphi_{Ti}) \cos(\theta_{Ti}) A_i}{\pi R_{Ti}^2} \rho_i \frac{\cos(\varphi_{ij}) \cos(\theta_{ij}) A_j}{\pi R_{ij}^2} \rho_j \frac{\cos(\varphi_{jR}) \cos(\theta_{jR}) A_R}{\pi R_{jR}^2} \delta\left(t - \frac{R_{Ti} + R_{ij} + R_{jR}}{c}\right) \quad (10)$$

Equation (10) makes it clear why received power through reflections becomes insignificant as higher

reflection orders are considered. This is the case, since n – th order impulse response is equal to $(n - 1)$ – th order multiplied by a quantity that is much smaller than one. In this study, up to a third reflection is considered in calculating the impulse response.

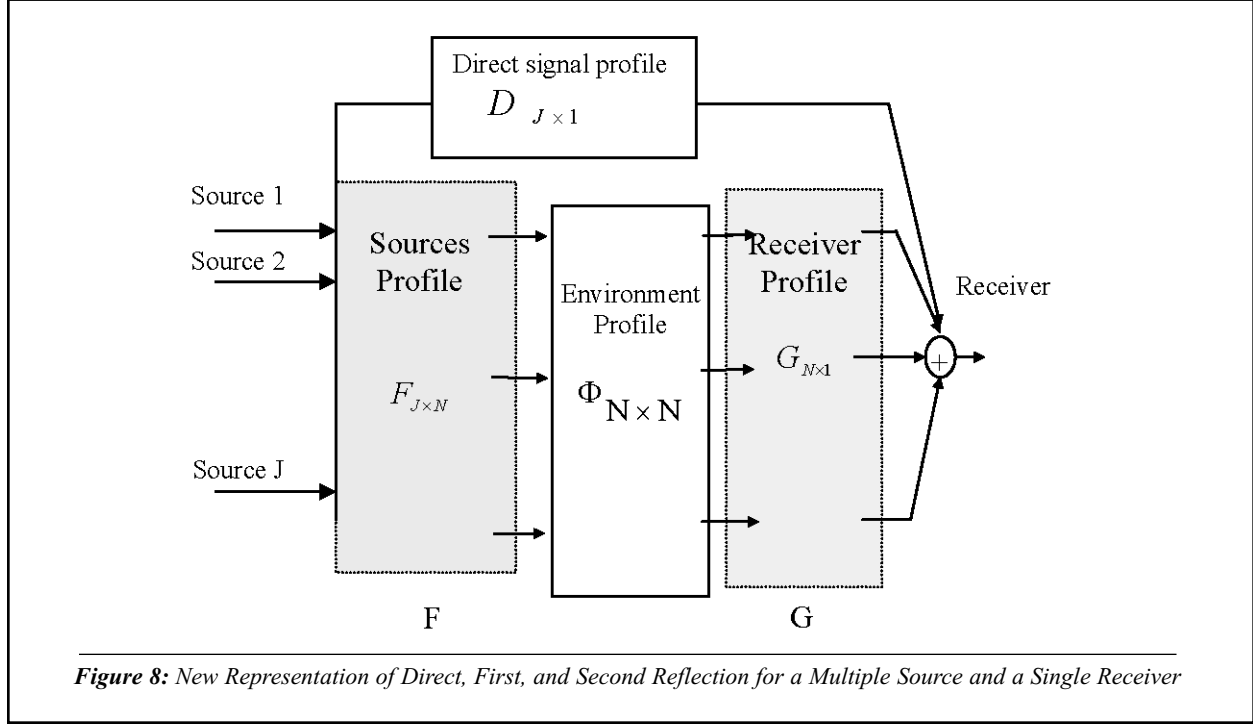
In this model, the transfer function between a transmitter and a receiver is divided into four components. The first represents the transfer function between sources and surface elements. The second block contains the transfer function between surface elements. The third has the transfer function from surface elements to a receiver. The last component accounts for direct response between a source and a receiver. These relations are presented in *Figure 8*.

The first component in this model represents transfer function between sources on the ceiling and surface elements. It is referred to as ‘‘Sources Profile’’ and is modeled by a multiple-input–multiple-output system with N outputs. The transfer function between each source and each of surface elements is expressed by an entry in matrix F .

The second component consolidates dependence on indoor geometry, dimensions, and reflection coefficients. This component contains the transfer functions between any two reflecting elements. In matrix format, and considering up to n reflections, it is expressed as

$$\Phi_n = \begin{cases} I_{N \times N} + \phi + \phi^2 + \phi^3 + \dots + \phi^{n-1} & , n \geq 2 \\ I_{N \times N} & , n = 1 \end{cases} \quad (11)$$

where $I_{N \times N}$ is the $N \times N$ identity matrix, and ϕ is given by



$$\phi = \begin{bmatrix} \phi_{11} & \cdots & \phi_{1N} \\ \vdots & \ddots & \vdots \\ \phi_{N1} & \cdots & \phi_{NN} \end{bmatrix} \quad (12)$$

The entry ϕ_{ik} represents transfer function between two elements i and k and is given by

$$\phi_{ik} = \begin{cases} 0 & , i = k \\ \frac{\rho_i \cos \theta_{ik} \cos \varphi_{ik} A_k}{\pi R_{ik}^2} \delta(t - \frac{R_{ik}}{c}) u(\frac{\pi}{2} - \theta_{ik}) & , i \neq k \end{cases} \quad (13)$$

The environment matrix is independent of transmitter and receiver, once calculated; it can be used with any transmitter-receiver configuration.

Receiver profile contains transfer functions between a receiver and N surface elements. In vector form, it is expressed as

$$G_r = \begin{bmatrix} g_{1r} \\ \vdots \\ g_{Nr} \end{bmatrix} \quad (14)$$

where the entry g_{ir} is given by

$$g_{ir} = \frac{\rho_i \cos \theta_{ir} \cos \varphi_{ir} A_r}{\pi R_{ir}^2} \delta(t - \frac{R_{ir}}{c}) u(FOV_r - \theta_{ir}) \quad (15)$$

Figure 9 shows the amplitude of G entries for different locations and FOV values. It is clear from the figure that the number of non-zero elements is directly proportional to the receiver FOV. The symmetry of the G vector is lost when the receiver is located close to more than one surface, each in a different plane.

When a source is within a receiver FOV, a direct response results. This response is expressed as

$$H^{(0)} = \sum_{i=1}^J d_i \quad (16)$$

where D is a $J \times 1$ vector given by

$$D = \begin{bmatrix} d_1 \\ \bullet \\ \bullet \\ \bullet \\ d_J \end{bmatrix} \quad (17)$$

The entry d_i 's are equal to $\frac{\cos \theta_{ir} \cos \varphi_{ir} A_r}{\pi R_{ir}^2} \delta(t - \frac{R_{ir}}{c}) u(FOV_r - \theta_{ir})$ and these correspond to J sources on the ceiling. R_{Ti} accounts for the delay between source i and receiver.

The total impulse response H between a source s and a receiver when n reflections are considered can be expressed as

$$H = \sum_{i=0}^n H^{(i)} = \sum_{i=1}^J d_i + F \cdot \Phi_n \cdot G_r \tag{18}$$

Following this modified method, we found the channel impulse response for two receivers at arbitrary points in our system: point A at (3, 2.5, 0.9) and point B at (0.5, 0.5, 0.9). The results are depicted in *Figure 9(a)* and *(b)*. For simulation purposes, we chose d to be equal 0.1 meter and the total number of points, N , equal to 14,400 points. The receiver specifications are those found earlier for reliable communications in our model room.

Other than reflections on the walls, optical path differences can cause a delay spread. These path differences are because of LOS–signal arrivals from different sources to a receiver. If a receiver at a certain point in the room has a large enough FOV to have more than one straight path to two or more transmitters, this receiver will capture strong signals from different transmitters with time delays. This phenomenon is seen in *Figure 10(a)*, where there are two significant strong signals in the estimated impulse response. The delay between these signals is given by *Equation (19)*.

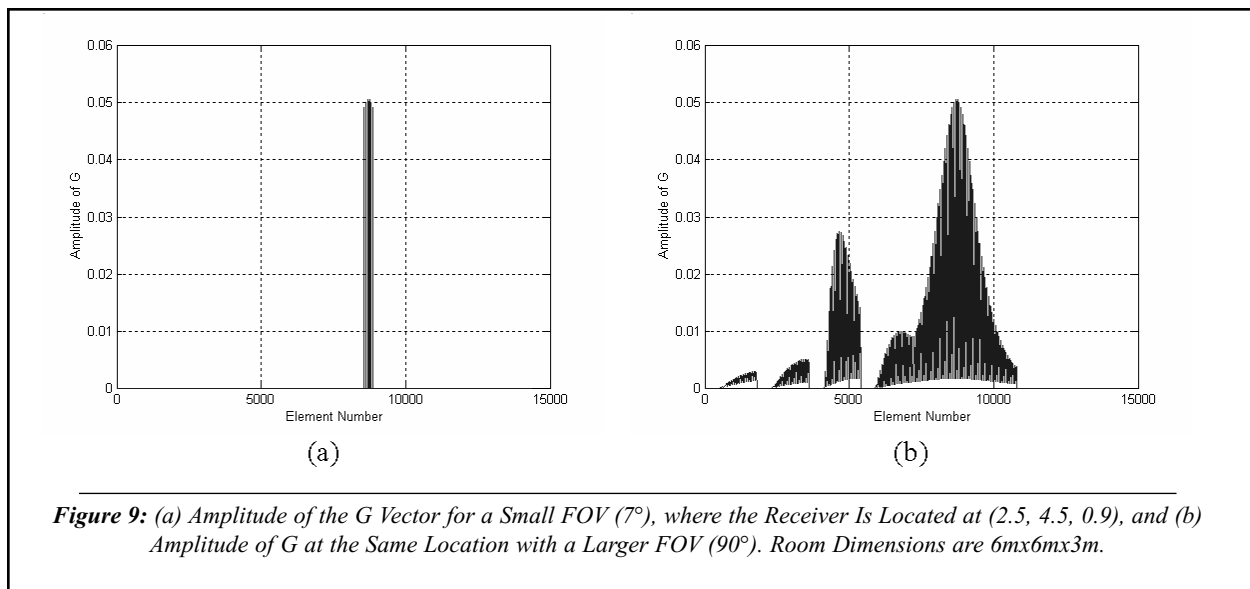
$$t_d = \frac{\sqrt{(w-x)^2 + h^2} - \sqrt{x^2 + h^2}}{c} \tag{19}$$

where c is the speed of light and w, x, h are shown in *Figure 11*.

With our room dimensions and the system configuration, a receiver, at most, can have an LOS path to two transmitters, and the worst delay between these two paths is one nanosecond. Therefore, in order to avoid a severe intersymbol interference (ISI), the transmission symbol rate needs to be less than one Giga symbols per second. This shows the superb transmission capacity of these channels. If the conventional on-off keying modulation is used, a bit rate of one Gbps is feasible.

Conclusions

This paper discusses the potential capabilities of two emerging technologies for broadband access: power-line communications and white-LED indoor communications. Our investigations showed power-line networks, either as medium- or low-voltage grids, could offer very high transmission capacities not achievable by any other wireline network except fiber. Furthermore, it is shown that the reflections caused by mismatches throughout the network degrade the performance of the system. Therefore, to attain a higher data rate, impedance matching in the power grid is necessary. If these



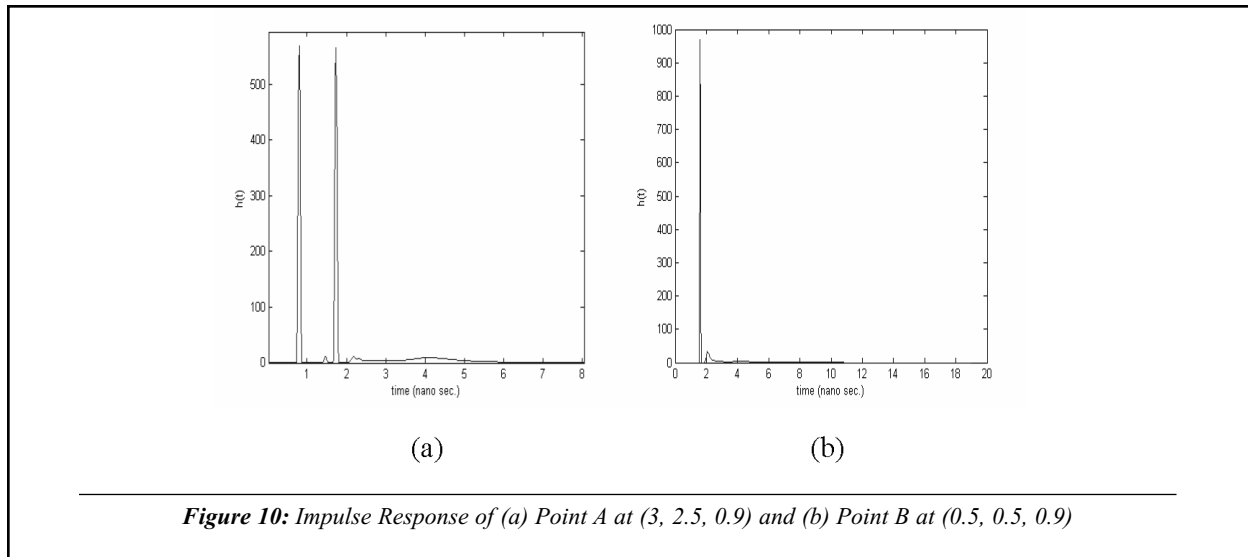


Figure 10: Impulse Response of (a) Point A at (3, 2.5, 0.9) and (b) Point B at (0.5, 0.5, 0.9)

networks are conditioned properly, a transmission rate as high as one Gbps will be feasible.

Moreover, we discussed the fundamental analysis of visible-light communication systems using white LEDs. These systems should provide optical lighting as well as optical transmission. To meet these criteria, we designed a white-LED system for lighting and high-data-rate indoor communications in a model room such that there is no blind spot in the room for data communications, while the room is lit almost uniformly. Next, we developed a channel model for the proposed system based on modeling algorithms provided in “MIMO characterization of indoor wireless optical link using a diffuse-transmission configuration.” It is shown that optical path difference can cause a signal distortion in high-

speed data transmission. This distortion is highly dependant on the room’s dimensions and system configuration. If a system is designed appropriately, this distortion can be minimized. For example, in our proposed system, at worst, distortion limits the data rates to one Gbps.

Our investigations showed that both systems could provide a very-high-data-rate communications access for indoor networking. Consequently, the integration of these two techniques will have an important effect as a new last-mile system.

References

1. P. Amirshahi and M. Kavehrad, “Transmission Channel Model and Capacity of Overhead Multi-conductor Medium-Voltage Power-lines for Broadband Communications,” IEEE Consumer Communications & Networking Conference, Las Vegas, Nevada, January 2005.
2. P. Amirshahi and M. Kavehrad, “Medium Voltage Overhead Power-line Broadband Communications: Transmission Capacity and Electromagnetic Interference,” PROCEEDINGS OF ISPLC 2005, Vancouver, Canada, April 2005.
3. T. Banwell and S. Galli, “A Novel Approach to the Modeling of the Indoor Power Line Channel – Part I: Circuit Analysis and Companion Model,” IEEE Transactions on Power Delivery, April 2005.
4. S. Galli, T. Banwell, “A Novel Approach to the Modeling of the Indoor Power Line Channel – Part II: Transfer Function and Its Properties,” IEEE Transactions on Power Delivery, April 2005.
5. G. Zorpette, “Let there be Light,” IEEE Spectrum, September 2002, 70–4.

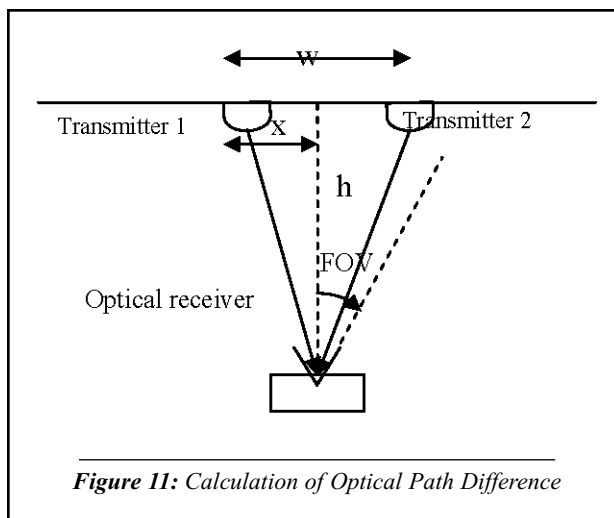


Figure 11: Calculation of Optical Path Difference

6. T. Komine, Y. Tanaka, S. Haruyama, and M. Nakagawa, "Basic study on visible light communications using Light emitting Diode Illumination," Proceedings of ISMOT 2001, Montreal, Canada, 2001, 45–8.
7. M. D'Amore and M.S. Sarto, "A New Formulation of Lossy Ground Return Parameters for Transient Analysis of Multi-conductor Dissipative Lines," *IEEE Transactions on Power Delivery*, Vol. 12, No.1, January 1997, 303–14.
8. Zimmerman M. and Dostert, K., "A multipath model for the power-line channel," *IEEE Transactions on Communications*, Vol. 50, No. 4, April 2002, 553–9.
9. Jae-Jo Lee, Seung-Ji Choi, Huy-Myoung Oh, Won-Tae Lee, Kwan-Ho Kim, and Dae-Young Lee, "Measurements of the Communications Environment in Medium Voltage Power Distribution Lines for Wide-band Power Line Communications," Proceedings of 2004 International Symposium on Power-line Communications and Its Applications, 2004, 69–74.
10. T. Komine and M. Nakagawa, "Fundamental analysis for visible light communications using LED lights," *IEEE Transactions on Consumer Electronics*, Vol. 50, No. 1, February 2004, 100–7.
11. S. Jivkova, B.A Hristov, M. Kavehrad, "Power-Efficient Multispot-Diffuse Multiple-Input–Multiple-Output Approach to Broadband Optical Wireless Communications," *IEEE Transactions on Vehicular Technologies*, Vol. 53, No. 3, May 2004, 882–9.
12. F.R Gfeller and U. Bapst, "Wireless in-house data communications via diffuse infra red radiation," Proceedings of IEEE, Vol. 67, No. 11, 1979, 14–74, 1486.
13. Y. Tanaka, S. Haruyama, and M. Nakagawa, "Wireless optical transmissions with white colored LED for wireless home links," Proceedings of PIMRC 2000, Vol. 2, September 2000, 1325–9.
14. Y. Alqudah and M. Kavehrad, "MIMO characterization of indoor wireless optical link using a diffuse-transmission configuration," *IEEE Transactions on Communications*, Vol. 59, No. 9, September 2003, 1554–60.
15. J. R. Barry, J. M. Kahn, W. J. Krause, E. A. Lee, and D. G. Messerschmitt, "Simulation of multipath impulse response for indoor wireless optical channels," *IEEE Journal on Selected Areas in Communications*, Vol. 11, No. 3, April 1993, 367–79.